Sterile Neutrinos in Light of Recent Cosmological and Oscillation Data: a Multi-Flavor Scheme Approach

Alessandro Melchiorri¹, Olga Mena², Sergio Palomares-Ruiz³, Silvia Pascoli⁴, Anze Slosar⁵ and Michel Sorel²

- 1 INFN Sez. di Roma, Dipartimento di Fisica, Universitá di Roma "La Sapienza", I-00185 Roma, Italy
- ² Instituto de Física Corpuscular, IFIC, CSIC and Universidad de Valencia, Spain
- ³ Centro de Física Teórica de Partículas, Instituto Superior Tecnico, 1049-001 Lisboa, Portugal
- $^{\rm 4}$ IPPP, Department of Physics, Durham University, Durham DH1 3LE, United Kingdom
- ⁵ Berkeley Center for Cosmological Physics, Physics Department and Lawrence Berkeley National Laboratory, University of California, Berkeley California 94720, USA

Abstract. Light sterile neutrinos might mix with the active ones and be copiously produced in the early Universe. In the present paper, a detailed multi-flavor analysis of sterile neutrino production is performed. Making some justified approximations allows us to consider not only neutrino interactions with the primeval medium and neutrino coherence breaking effects, but also oscillation effects arising from the presence of three light (mostly-active) neutrino states mixed with two heavier (mostly-sterile) states. First, we emphasize the underlying physics via an analytical description of sterile neutrino abundances that is valid for cases with small mixing between active and sterile neutrinos. Then, we study in detail the phenomenology of (3+2) sterile neutrino models in light of short-baseline oscillation data, including the LSND and MiniBooNE results. Finally, by using the information provided by this analysis, we obtain the expected sterile neutrino cosmological abundances and then contrast them with the most recent available data from Cosmic Microwave Background and Large Scale Structure observations. We conclude that (3+2) models are significantly more disfavored by the internal inconsistencies between sterile neutrino interpretations of appearance and disappearance short-baseline data themselves, rather than by the used cosmological data.

Submitted to: Journal of Cosmology and Astroparticle Physics

PACS numbers: 14.60.Pq, 98.80.-k

1. Introduction

During the last several years the physics of neutrinos has achieved remarkable progress. The experiments with solar [1, 2, 3, 4, 5, 6], atmospheric [7, 8], reactor [9], and also accelerator neutrinos [10, 11, 12], have provided compelling evidence for the existence of neutrino oscillations, implying non-zero neutrino masses.

The present data require at least two large (θ_{12} and θ_{23}) angles in the neutrino mixing matrix and at least two mass squared differences, $\Delta m_{ji}^2 \equiv m_j^2 - m_i^2$ (where m_j 's are the neutrino masses), one driving the atmospheric (Δm_{31}^2) and the other one the solar (Δm_{21}^2) neutrino oscillations. The mixing angles θ_{12} and θ_{23} control the solar and the atmospheric neutrino oscillations, while the third angle θ_{13} in the three neutrino mixing matrix is bound to be small by the data from the CHOOZ and Palo Verde reactor experiments [13, 14]. Unfortunately, oscillation experiments only provide bounds on the neutrino mass squared differences, i.e. they are insensitive to the overall neutrino mass scale.

Cosmology provides one of the means to tackle the absolute scale of neutrino masses. The Universe can be thus exploited as a new laboratory where to test neutrino masses and neutrino physics. The new accurate measurements of the Cosmic Microwave Background (CMB) anisotropy and polarization from satellite, balloon-borne and ground-based experiments have fully confirmed the predictions of the standard cosmological model (see e.g. [15]) and allow us to weigh neutrinos. Neutrinos can indeed play a relevant role in large scale structure formation and leave key signatures in several cosmological data sets. More specifically, the amount of primordial relativistic neutrinos change the epoch of the matter-radiation equality, leaving an imprint on both CMB anisotropies (through the so-called Integrated Sachs-Wolfe effect) and on structure formation, while non relativistic neutrinos in the recent Universe suppress the growth of matter density fluctuations and galaxy clustering (see e.g [16]).

All these new observations have allowed us to place new bounds on neutrino physics from cosmology [17, 18, 19, 15, 20, 22, 23] constraining the amount of energy density in neutrinos and their mass, in the framework of three active degenerate neutrinos, to be below $\sim 0.25 \, \mathrm{eV}$ at 95% C.L. However, the three neutrino scenario is a minimal scheme, inspired, following a theoretical prejudice, by a model which tries to resemble the three family structure of quarks and charged leptons. We now know neutrinos are different from the quark and charged lepton sectors and there is no fundamental symmetry in nature forcing a definite number of right-handed (sterile) neutrino species, as those are allowed in the Standard Model fermion content.

Models with three active neutrinos plus an additional sterile one (3+1 models) were introduced [24] to explain simultaneously solar, atmospheric and LSND [25] data. The mass of a fourth, thermal, sterile neutrino has been constrained from cosmological data to be less than $\sim 0.65 \text{ eV}$ at 95% C.L. (see e.g. [19]). While cosmological constraints on the neutrino mass are certainly remarkable, one should be careful in taking those constraints blindly, since they are obtained in a model-dependent way. For instance,

the constraint on the mass of the fourth sterile neutrino presented in [19] is obtained under the assumption of a (3+1) scenario with a fully thermalized sterile neutrino. On the other hand, if different thermalization mechanisms are considered [26, 27, 28, 29], the cosmological constraints on neutrino masses could be relaxed or even drastically changed.

More recently, scenarios with three active plus two sterile neutrinos (3 + 2 models) [30] have been shown to provide a better fit to short baseline (SBL) data compared to (3 + 1) models [31, 32, 33], since they can, within a neutrino oscillation framework, bring into agreement the LSND $\bar{\nu}_e$ excess in a $\bar{\nu}_{\mu}$ beam [25] and the null results from other SBL oscillation experiments. The masses for the additional mostly-sterile neutrinos we are interested in are much larger than the light neutrino ones, $m_4, m_5 \gg m_1, m_2, m_3$. Throughout this paper, we take the convention $m_5 > m_4$. The flavor neutrino base ν_{α} , $\alpha = e, \mu, \tau, s, p$, is related to the massive base ν_i , i = 1, 2, 3, 4, 5, through a 5 × 5 unitary matrix which we indicate as U:

$$\nu_{\alpha} = U_{\alpha i} \nu_{i} . \tag{1}$$

Searches of sterile neutrinos indicate that the mixing between heavy neutrinos and active neutrinos and between light neutrinos and sterile ones is very small, so throughout our study we will take $|U_{a4}|$, $|U_{a5}|$, $|U_{js}|$, $|U_{jp}| \ll 1$, with $a = e, \mu, \tau$ and j = 1, 2, 3.

The way in which these neutrinos shape the Universe depends crucially on the thermalization processes. The purpose of the present study is to test the cosmological viability of the (3 + 2) scenario in which sterile neutrinos are produced through oscillations [34, 35, 36, 37, 38, 39, 40, 41, 42] (see [43, 44, 45] for earlier works), applying a multi-flavor treatment in the evolution of the system. We add in the analysis the most recent neutrino oscillation data, which includes the first MiniBooNE $\nu_{\mu} \rightarrow \nu_{e}$ oscillation results. Finally, let us note that the presence of additional relativistic degrees of freedom at the epoch of Big Bang Nucleosynthesis (BBN) modifies significantly the production of helium, deuterium and lithium (a recent review is given in [46], see also [47]), so this observational data on the abundance of light elements allows one to put severe constraints on sterile neutrino parameters. However, in the present study we consider the contribution of sterile neutrinos to the energy density of the Universe and its effects on the CMB and on the matter power spectrum, but we do not include the data from BBN observations.

The structure of the paper is as follows. In Sec. 2 we describe the sterile neutrino production. Although we do not attempt to solve the exact quantum kinetic equations for a (3+2) system, we have numerically computed the momentum-averaged counterpart with an approximation for the coherence-breaking terms. This amounts to solve an equation for the 5×5 (anti)neutrino density matrix in order to use these solutions in our Markov chain Monte Carlo (MCMC) analyses. We present as well an analytical approach which, under a number of approximations, describes the neutrino thermalization in a multi-family scenario, deriving very simple formulae that illustrate the evolution process in a very clear way. Sec. 3 describes the SBL oscillation data and the cosmological data

sets used in the MCMC analyses. We present our results in Sec. 4, discussing first the compatibility of oscillation and cosmological data and presenting afterwards a combined analysis of both data sets. We conclude in Sec. 5.

2. Sterile Neutrino Production in the Multi-Flavor Approach

As a case study of sterile neutrino cosmological abundance in multi-flavor schemes, we consider mixings among three active plus two sterile neutrino states, i.e., the so-called (3+2) sterile neutrino models. In the Early Universe, and in particular for temperatures above neutrino decoupling (T>1 MeV), neutrinos are part of a gas of interacting multispecies of elementary particles. In this environment, sterile neutrinos can be produced via the oscillations of active neutrinos in presence of interactions with the thermal plasma (for foundational work see [43, 48, 49, 50, 51, 52, 53, 54, 55, 56]). Due to the high temperatures, the neutrino mean free path is quite small and it is essential to take into account the breaking of coherence, using the density matrix formalism. The quantum operator for the density matrix of neutrinos is defined as $\hat{\rho}_j^i = \nu^i \nu_j^*$. The C-valued density matrix, $\rho(E,T)$, is obtained by taking the average of the matrix element over the medium. Although the exact form of the terms which take into account the loss of coherence is quite complicated [51, 53, 54, 56, 57], a good approximate treatment is obtained if the kinetic equations for ρ are written as in [58] (where we will omit writing the E and T dependence in what follows):

$$\dot{\rho} = i \left[H_{\rm m} + V_{\rm eff}, \rho \right] - \left\{ \Gamma, (\rho - \rho_{\rm ed}) \right\} . \tag{2}$$

Here, $H_{\rm m} = U H_0 U^{\dagger}$ is the free neutrino Hamiltonian in the flavor basis, which is obtained rotating the Hamiltonian in the mass basis $H_0 = {\rm diag}(E_1, E_2, E_3, E_4, E_5)$ by the unitary mixing matrix U given by Eq. (1). For the temperatures under consideration, neutrinos are highly relativistic and the approximation $E = p + m^2/(2p)$, with $p(\simeq E)$ the neutrino momentum, holds and will be applied. The effective potential $V_{\rm eff}$ describes the interactions of neutrinos with the medium and is diagonal in the flavor basis. For negligible lepton asymmetry, its elements are approximately given by:

$$V_{\text{eff},a} = -C_a G_F^2 T^4 E/\alpha , \qquad (3)$$

where G_F is the Fermi coupling constant, T is the plasma temperature, E is the neutrino energy, $\alpha = 1/137$ the fine structure constant. The constants C_a are given by $C_e \sim 0.61$ and $C_{\mu,\tau} \sim 0.17$ (for $T < m_{\mu}$) [59], which are exact in the limit of thermal equilibrium of all leptons involved, and sufficiently accurate for our purposes. The coherence loss in the evolution of the non-diagonal terms is given by $\dot{\rho} = -\Gamma \rho$ [43, 51, 40, 54] and a simplified but accurate way to describe the neutrino production and destruction is given by the anticommutator term in Eq. (2) [58]. The damping factor Γ is diagonal in the flavor basis, $\Gamma = \text{diag}(\Gamma_e, \Gamma_{\mu}, \Gamma_{\tau}, 0, 0)$, and its elements, taking the total scattering rate, in the Boltzmann approximation [40], are given by:

$$\Gamma_a = g_a \frac{90 \zeta(3)}{7 \pi^4} G_F^2 T^4 p , \qquad (4)$$

with $a = e, \mu, \tau$. The coefficients g_a have been computed numerically and are given by $g_e \simeq 3.6$, $g_{\mu} = g_{\tau} \simeq 2.5$ [60]. The diagonal matrix $\rho_{eq} = \text{diag}(\rho_{eq}) = I(\exp(E/T) + 1)^{-1}$, with I the identity matrix, is the equilibrium value of the density matrix.

For the purpose of this work we can assume that, in the range of temperatures under interest, the time dependence of the temperature scales as $\dot{T} \simeq -HT$, where H is the Hubble expansion rate. Using the fact that

$$T\left(\frac{\partial\rho}{\partial T}\right)_{E} + E\left(\frac{\partial\rho}{\partial E}\right)_{T} = T\left(\frac{\partial\rho}{\partial T}\right)_{\frac{E}{T}},\tag{5}$$

we can rewrite Eq. (2) as

$$\left(\frac{\partial \rho}{\partial T}\right)_{\frac{E}{T}} \simeq -\frac{1}{HT} \left(i\left[H_{\rm m} + V_{\rm eff}, \rho\right] - \left\{\Gamma, (\rho - \rho_{\rm eq})\right\}\right), \tag{6}$$

where

$$H(T) = \sqrt{\frac{4\pi^3 g_{\star}}{45}} \frac{T^2}{m_{Pl}} \,. \tag{7}$$

Here, m_{Pl} is the Planck mass, while g_{\star} is the number or relativistic degrees of freedom. In the range of temperatures where all the processes we are interested in take place, g_{\star} changes very little. Hence, we have neglected the temperature dependence of g_{\star} in the time dependence of the temperature, although we have taken it into account in the expression of the Hubble rate.

The MCMC analyses presented in Sec. 3 use the solutions to the approximate evolution equation, Eq. (6), for the 5×5 (anti)neutrino density matrix ρ . Given the hermiticity of the C-valued density matrix, this amounts to solving a set of 30 coupled first-order differential equations. Thus, in order to reduce the computing load, to solve Eq. (6), we only consider monoenergetic neutrinos at any given temperature, taking an average value of $E = 7\zeta(4)T/(2\zeta(3)) \simeq 3.15\,T$. In general, if the oscillations are faster than the Universe expansion rate as is the case, this is a justified approximation [56]. On the other hand, we take thermal abundances for the mostly-active neutrino triplet and zero abundances for the mostly-sterile states, as initial conditions at a temperature of $T \sim 100$ MeV, and follow the temperature evolution until T = 1 MeV ‡. As a further approximation, we assume active neutrinos keep perfect thermal distribution throughout the evolution. This is justified as any active neutrino population depleted due to oscillations will be immediately repopulated thanks to its interaction with the plasma. Furthermore, if there is no neutrino-antineutrino asymmetry as we are assuming, active-active oscillations must have no effect at all [45, 56].

In the following, Sec. 2.1, we present an analytical description of the solutions to Eq. (6), providing formulas for sterile neutrino production in the Early Universe that are very good approximations for sterile neutrino scenarios with small mixings among active and heavy neutrinos (and among sterile and light neutrinos). We will use these results to show the effects of different approximations assumed when solving numerically the problem.

‡ Note that post weak decoupling effects can only be important when there is a large lepton number [61].

2.1. Analytical Description

The production of sterile neutrinos can be computed by solving Eq. (2) and in particular by following the evolution of the diagonal sterile terms ρ_{ss} and ρ_{pp} . In the present analytical derivation, we are interested in values of the heavy sterile masses such that $\Delta m_{41}^2, \Delta m_{51}^2 \gg \Delta m_{31}^2, \Delta m_{21}^2$ and small mixing between the active and heavy sectors and between the sterile and light sectors. In this case, sterile neutrinos never reach complete thermalization and their abundances are much lower than the equilibrium one.

As mentioned above, the resolution of Eq. (2) implies solving a system of 30 coupled first-order differential equations. However as the typical frequency for oscillations between active (ν_a , $a = e, \mu, \tau$) and sterile (ν_h , h = s, p) neutrinos, given by

$$\omega_{ah} = \sqrt{\sum_{i} \left(\frac{\Delta m_{i1}^{2} U_{ai} U_{hi}^{*}}{E}\right)^{2} + \left(\sum_{i} \frac{\Delta m_{i1}^{2} (|U_{ai}|^{2} - |U_{hi}|^{2})}{2E} + V_{\text{eff},a}\right)^{2}}, \quad (8)$$

is much larger than the expansion rate of the Universe H in the epoch when sterile neutrino production takes place, we can use the static approximation [62, 57]:

$$\dot{\rho}_{ah} = 0 , \qquad (9)$$

$$\dot{\rho}_{sp} = 0 . \tag{10}$$

All the off-diagonal terms can be found by solving this system of 20 coupled linear equations. Hence, this approximation reduces the problem to the resolution of a system of 5 coupled first-order differential equations, involving only the diagonal elements of the density matrix, which is given by

$$\dot{\rho}_{\alpha\alpha} = 2 \left[\sum_{\beta \neq \alpha} \operatorname{Im} \left(H_{\alpha\beta}^* \rho_{\alpha\beta} \right) - \Gamma_{\alpha} \left(\rho_{\alpha\alpha} - \rho_{eq} \right) \right] , \quad \alpha, \beta = e, \mu, \tau, s, p \quad (11)$$

where we have defined:

$$H_{\alpha\beta} \equiv \sum_{i} \frac{\Delta m_{i1}^{2}}{2E} U_{\alpha i} U_{\beta i}^{*} + V_{\text{eff},\alpha} \delta_{\alpha\beta} , \qquad (12)$$

with $V_{\text{eff},a}$ given by Eq. 3, and $V_{\text{eff},s}, V_{\text{eff},p} = 0$.

For the small mixing case considered, production of sterile neutrinos never reaches thermal abundances, i.e., $\rho_{ss}, \rho_{pp} \ll \rho_{eq}$, and the effects on the active neutrino distribution are very small and therefore we can use the approximation $\rho_{aa} \simeq \rho_{eq}$ §. This simplifies further the problem and, using the fact that $H_{a\beta} \ll H_{sp}, H_{ss}, H_{pp}$ holds in this case, with $\beta = e, \mu, \tau, s, p$, the remaining three systems of four linear equations corresponding to Eqs. (9), one system for each active neutrino, can be solved to find:

$$\rho_{as} \simeq \rho_{eq} \frac{H_{as} (H_{aa} - H_{pp} + i\Gamma_a) + H_{ap} H_{sp}^*}{(H_{aa} - H_{ss} + i\Gamma_a) (H_{aa} - H_{pp} + i\Gamma_a) - |H_{sp}|^2} , \tag{13}$$

$$\rho_{ap} \simeq \rho_{eq} \frac{H_{ap} (H_{aa} - H_{ss} + i\Gamma_a) + H_{as} H_{sp}}{(H_{aa} - H_{ss} + i\Gamma_a) (H_{aa} - H_{pp} + i\Gamma_a) - |H_{sp}|^2} . \tag{14}$$

§ Note that we will also use this approximation for larger mixings, as those studied below. Even in that case, the distortion of the active neutrino distribution is small enough for our purposes and is not expected to alter substantially our results.

Although ρ_{sp} turns out to be subdominant with respect to ρ_{as} , it plays a relevant role in the evolution of ρ_{ss} and ρ_{pp} and cannot be neglected. From Eq. (10), we get:

$$\rho_{sp} \simeq \rho_{eq} \frac{\sum_{a} \left(\rho_{as}^* H_{ap} - \rho_{ap} H_{as}^* + H_{sp} (\rho_{ss} - \rho_{pp}) \right)}{H_{ss} - H_{pp}} . \tag{15}$$

In the approximations we made, the evolution of ρ_{ss} and ρ_{pp} can be explicitly given by:

$$\dot{\rho}_{ss} = -2 \operatorname{Im} \left(\sum_{a} \rho_{as} H_{as}^* - \rho_{sp} H_{sp}^* \right) , \qquad (16)$$

$$\dot{\rho}_{pp} = -2 \operatorname{Im} \left(\sum_{a} \rho_{ap} H_{ap}^* + \rho_{sp} H_{sp}^* \right) . \tag{17}$$

By substituting the expressions for ρ_{ah} in Eqs. (13) and (14) and ρ_{sp} in Eq. (15), one can obtain the two differential equations for ρ_{ss} and ρ_{pp} which can then be solved in order to find the sterile neutrino abundance in the Early Universe. It is interesting to notice that the terms proportional to ρ_{ss} and ρ_{pp} in the imaginary part in the r.h.s. of Eqs. (16) and (17) are real as they are proportional to $|H_{sp}|^2$ and therefore vanish. This implies that the system is now given by two uncoupled differential equations which can be solved either numerical or analytically with some approximations.

For a real mixing matrix, which will hold in the numerical study we will perform later, the results are simplified and the evolution of ρ_{ss} and ρ_{pp} depends only on the imaginary part of the off-diagonal elements of the density matrix $\rho_{h\beta}$, h = s, p, as:

$$\dot{\rho}_{hh} = -2 \left[\sum_{\beta \neq h} H_{h\beta} \operatorname{Im}(\rho_{\beta h}) \right] , \quad \beta = e, \mu, \tau, s, p$$
(18)

which we will use throughout the remaining of this section. For compactness of notation, we define

$$I_{\alpha\beta} \equiv \operatorname{Im}(\rho_{\alpha\beta}) = -\operatorname{Im}(\rho_{\beta\alpha}) \ .$$
 (19)

From Eqs. (13) and (14), we can find the explicit form of I_{as} and I_{ap} :

$$I_{as} \simeq -\left[\frac{\left[\left(H_{aa} - H_{pp}\right)^{2} + \Gamma_{a}^{2} + H_{sp}^{2}\right] H_{as}}{D} + \frac{\left[\left(H_{aa} - H_{ss}\right) + \left(H_{aa} - H_{pp}\right)\right] H_{sp} H_{ap}}{D}\right] \Gamma_{a} \rho_{eq} , \qquad (20)$$

$$I_{ap} \simeq -\left[\frac{\left[\left(H_{aa} - H_{ss}\right)^{2} + \Gamma_{a}^{2} + H_{sp}^{2}\right] H_{ap}}{D} + \frac{1}{2} \left[\frac{\left(H_{aa} - H_{ss}\right)^{2} + \Gamma_{a}^{2} + H_{sp}^{2}\right] H_{ap}}{D} + \frac{1}{2} \left[\frac{\left(H_{aa} - H_{ss}\right)^{2} + \Gamma_{a}^{2} + H_{sp}^{2}\right] H_{ap}}{D} + \frac{1}{2} \left[\frac{\left(H_{aa} - H_{ss}\right)^{2} + \Gamma_{a}^{2} + H_{sp}^{2}\right] H_{ap}}{D} + \frac{1}{2} \left[\frac{\left(H_{aa} - H_{ss}\right)^{2} + \Gamma_{a}^{2} + H_{sp}^{2}\right] H_{ap}}{D} + \frac{1}{2} \left[\frac{\left(H_{aa} - H_{ss}\right)^{2} + \Gamma_{a}^{2} + H_{sp}^{2}\right] H_{ap}}{D} + \frac{1}{2} \left[\frac{\left(H_{aa} - H_{ss}\right)^{2} + \Gamma_{a}^{2} + H_{sp}^{2}}{D}\right] H_{ap}}{D} + \frac{1}{2} \left[\frac{\left(H_{aa} - H_{ss}\right)^{2} + \Gamma_{a}^{2} + H_{sp}^{2}}{D}\right] H_{ap}}{D} + \frac{1}{2} \left[\frac{\left(H_{aa} - H_{ss}\right)^{2} + \Gamma_{a}^{2} + H_{sp}^{2}}{D}\right] H_{ap}}{D} + \frac{1}{2} \left[\frac{\left(H_{aa} - H_{ss}\right)^{2} + \Gamma_{a}^{2} + H_{sp}^{2}}{D}\right] H_{ap}}{D} + \frac{1}{2} \left[\frac{\left(H_{aa} - H_{ss}\right)^{2} + \Gamma_{a}^{2} + H_{sp}^{2}}{D}\right] H_{ap}}{D} + \frac{1}{2} \left[\frac{\left(H_{aa} - H_{ss}\right)^{2} + \Gamma_{a}^{2} + H_{sp}^{2}}{D}\right] H_{ap}}{D} + \frac{1}{2} \left[\frac{\left(H_{aa} - H_{sp}\right)^{2} + \Gamma_{a}^{2} + H_{sp}^{2}}{D}\right] H_{ap}}{D} + \frac{1}{2} \left[\frac{\left(H_{aa} - H_{sp}\right)^{2} + \Gamma_{a}^{2} + H_{sp}^{2}}{D}\right] H_{ap}}{D} + \frac{1}{2} \left[\frac{\left(H_{aa} - H_{sp}\right)^{2} + \Gamma_{a}^{2} + H_{sp}^{2}}{D}\right] H_{ap}}{D} + \frac{1}{2} \left[\frac{\left(H_{aa} - H_{sp}\right)^{2} + \Gamma_{a}^{2} + H_{sp}^{2}}{D}\right] H_{ap}}{D} + \frac{1}{2} \left[\frac{\left(H_{aa} - H_{sp}\right)^{2} + H_{sp}^{2}}{D}\right] H_{ap}}{D} +$$

$$\frac{[(H_{aa} - H_{pp}) + (H_{aa} - H_{ss})] H_{sp} H_{as}}{D} \Gamma_a \rho_{eq} , \qquad (21)$$

where

$$D \equiv \left[(H_{aa} - H_{pp}) (H_{aa} - H_{ss}) - H_{sp}^{2} \right]^{2} + \tag{22}$$

$$\Gamma_a^2 \left[(H_{aa} - H_{ss})^2 + (H_{aa} - H_{pp})^2 + 2 H_{sp}^2 \right] + \Gamma_a^4$$
 (23)

Finally, from Eq. (15), the element I_{sp} can be further expressed in terms of the six I_{ah} ,

$$I_{sp} \simeq -\frac{1}{H_{ss} - H_{pp}} \sum_{a} (H_{ap}I_{as} + H_{as}I_{ap})$$
 (24)

Note that, as already discussed for the general complex case, I_{sp} turns out to be subdominant with respect to I_{ah} , as it is suppressed by $H_{ah}/(H_{ss}-H_{pp})$. However, as it is clear from Eq. (18), it can play a relevant role in the evolution of ρ_{ss} and ρ_{pp} . In that equation, whereas the prefactor of I_{ah} is H_{ah} , that of I_{sp} is H_{sp} , which can compensate the smallness of I_{sp} with respect to I_{ah} . Hence, whenever there is mixing between the two sterile states, I_{sp} must be taken into account. It is important to note that I_{as} , I_{as} and I_{as} are proportional to Γ_a , indicating that the production of sterile neutrinos in the Early Universe is due to the breaking of coherence in the evolution of active neutrinos.

Using the approximation that the time-dependence of the temperature scales as $\dot{T} \simeq -HT$ and Eq. (5), we can rewrite Eqs. (18)-(24) as:

$$HT\left(\frac{\partial \rho_{ss}}{\partial T}\right)_{\frac{E}{T}} \simeq 2\sum_{a} H_{as} I_{as} - 2H_{sp} I_{sp} ,$$
 (25)

$$HT \left(\frac{\partial \rho_{pp}}{\partial T}\right)_{\frac{E}{T}} \simeq 2\sum_{a} H_{ap} I_{ap} + 2H_{sp} I_{sp}$$
 (26)

This is the system of two uncoupled first-order differential equations which has to be solved. Indeed obtaining the final abundance of sterile neutrinos can be easily performed numerically.

In addition, in the case of no mixing in the sterile sector as we are considering in this work, i.e., U_{s5} , $U_{p4} \ll 1$ ($H_{sp} \simeq 0$), Eqs. (20) and (21) further simplify (with h = s or p) to:

$$I_{ah} \simeq -\frac{H_{ah}}{(H_{aa} - H_{hh})^2 + \Gamma_a^2} \Gamma_a \rho_{\text{eq}} ,$$
 (27)

and ρ_{hh} is given from Eqs. (25) and (26) by

$$\frac{\rho_{hh}}{\rho_{\text{eq}}} \simeq \int_{T_{\text{dec}}}^{\infty} \frac{1}{HT} \sum_{a} \frac{H_{ah}^2}{\left(H_{aa} - H_{hh}\right)^2 + \Gamma_a^2} \Gamma_a dT \tag{28}$$

where E/T is kept constant. Here, $T_{\rm dec}$ is the decoupling temperature of the active neutrinos, which is of few MeV, depending on flavor. The term Γ_a^2 in the denominator can be neglected as this gives a small relative correction to the final value of the sterile neutrino distribution of order $(\Gamma_a/V_a)^2 \sim 10^{-4}$. Using this, we can rewrite Eq. (28), keeping only the dominant terms and substituting numerical factors, as

$$\frac{\rho_{hh}}{\rho_{\text{eq}}} \simeq 0.053 \, y \, \left(\frac{\Delta m_{j1}^2}{\text{eV}^2}\right)^2 \, \frac{U_{hj}^2}{\sqrt{g_{\star}}} \, \sum_a g_a \, U_{aj}^2 \, \int_{x_{\text{dec}}}^{\infty} \, \frac{dx}{\left(\frac{\Delta m_{j1}^2}{\text{eV}^2} \, U_{hj}^2 + 3.7 \times 10^{-8} \, C_a \, x^2 \, y^2\right)^2} (29)$$

where $x \equiv (T/\text{MeV})^3$ ($x_{\text{dec}} \equiv (T_{\text{dec}}/\text{MeV})^3$), $y \equiv E/T$ and j = 4(5) for h = s(p). This is the same integral which appears when solving the simplified two-neutrino case [42].

A further simplification can be applied by taking into account that, for the values of Δm_{41}^2 and Δm_{51}^2 we are interested in ($\gtrsim \mathcal{O}(1~\text{eV}^2)$), the maximum of production of sterile neutrinos happens at $T_{\text{max}} \simeq 13~\text{MeV} \left(\Delta m_{j1}^2/\text{eV}^2\right)^{1/6}$ [34, 36, 38, 42, 58] and thus $T_{\text{max}}^3 \gg T_{\text{dec}}^3$, so the lower limit of integration can be safely put to 0. The relative error introduced is of order $T_{\text{dec}}^3 G_F E/T \sqrt{C_a/(\alpha \Delta m_{j1}^2)} \sim 10^{-3} \sqrt{1~\text{eV}^2/\Delta m_{j1}^2}$. With these approximations the integral can be performed analytically and the final sterile neutrino distribution is given by:

$$\frac{\rho_{hh}}{\rho_{eq}} \simeq 6.6 \times 10^{-3} \sqrt{\frac{\Delta m_{j1}^2}{\text{eV}^2}} \sum_a \frac{g_a}{\sqrt{C_a}} \left(\frac{U_{aj}}{10^{-2}}\right)^2$$
 (30)

where we have taken $g_{\star} = 10.75$ and $U_{hj} \simeq 1$. It should be noticed that for large values of $U_{aj} \ (\gtrsim 10^{-2})$, the sterile neutrino distribution approaches the equilibrium value and our results are not valid anymore.

As $\rho_{hh}(E,T)$ has the same functional form as $\rho_{eq}(E,T)$, it is straightforward to obtain the contribution to the energy density of the Universe of each of the heavy states, which is simply given by

$$\Omega_h h^2 \simeq 7 \times 10^{-5} \left(\frac{\Delta m_{j1}^2}{\text{eV}^2} \right) \sum_a \frac{g_a}{\sqrt{C_a}} \left(\frac{U_{aj}}{10^{-2}} \right)^2$$
(31)

We reiterate that the results in Eqs. (30) and (31) are only valid for ρ_{ss} , $\rho_{pp} \ll \rho_{eq}$. It is straightforward to recover the well-known two-neutrino results from these expressions, which as one could expect, indicate that in the case of no mixing between the sterile states, the calculation of each of the heavy neutrino abundances reduces to adding the individual contributions due to their mixing with each of the active neutrinos.

2.2. Accuracy of approximations

As mentioned above, we do not attempt to solve the exact quantum kinetic equations for a (3+2) system, but instead numerically find the momentum-averaged solutions for the simplified counterpart given by Eq. (6). This approach describes the loss of coherence in an approximate way which, along with the assumption of monochromaticity, allows us to reduce the integro-differential system into a system of first-order differential equations.

It is well known that the averaging over momentum is a justified approximation if the relative oscillation phases can be ignored, as is the case if oscillations are not slower than the expansion rate of the Universe [56]. On the other hand, it has also been shown [58] that a reasonably accurate description of the coherence loss can be achieved by making use of the anticommutator in Eq. (6).

Keeping in mind that our starting point is not the system of exact equations but an approximate one, we discuss some further approximations assumed in order to be able to fully solve the system of 30 coupled first-order differential equations and study what is their effect on the final result. In order to do so, we consider the analytic calculation described above for the small mixing case.

Among the different approximations used, there is the monochromaticity of the neutrinos, assuming that active neutrinos are always in equilibrium, neglecting the

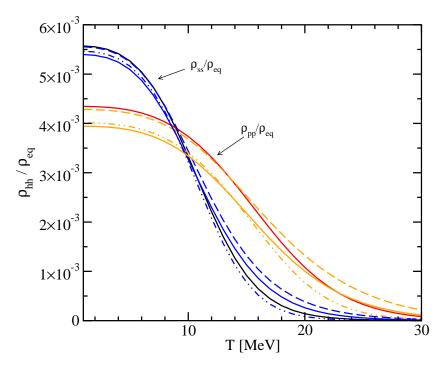


Figure 1. Ratios ρ_{ss}/ρ_{eq} and ρ_{pp}/ρ_{eq} as a function of the temperature as given by Eq. (28) with all approximations (see text) and when only some of these approximations are implemented. The black (red) solid lines refer to the case when all approximations are taken to obtain ρ_{ss} (ρ_{pp}). The blue (orange) lines represent solutions to ρ_{ss} (ρ_{pp}) with some approximations taken more accurately; dashed lines refer to the case when the momentum spread is taken into account, dot-dashed lines to the case when the exact form of the effective potential is considered and solid lines represent the case when both the momentum spread and the exact potential are assumed. The parameters we have taken are: $U_{e4} = U_{\mu 4} = 2 \times 10^{-3}$, $U_{e5} = U_{\mu 5} = 10^{-3}$, $m_4 = 1$ eV and $m_5 = \sqrt{10}$ eV.

temperature dependence of the number of degrees of freedom (g_{\star}) and using an approximate expression for the effective potential.

We find that the most important effect when sterile neutrinos are close to equilibrium is due to neglecting the change of the number of degrees of freedom as they get produced. Obviously, this approximation has a negligible effect in the small mixing case. Surprisingly, however, the effect of not taking into account the departure from equilibrium of the leptons as the temperature decreases, i.e., using an approximate expression for the effective potential, is comparable to the previous one even in the case of small mixing. On the other hand, we have explicitly checked for various cases that, as expected, solving for an averaged momentum introduces a very small error.

To conclude, these approximations tend to overestimate the final abundance, although none of them induces an error larger than $\sim 10\%$. This is depicted in Fig. 1, where we show the effect of two of these approximations in the case of small mixings by solving Eq. (28). The black (red) solid lines represent the solution for ρ_{ss} (ρ_{pp}) when all approximations are implemented. By removing these approximations, we show their

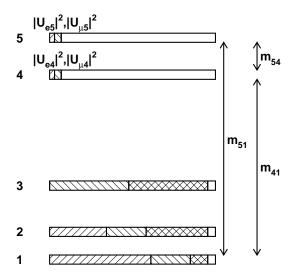


Figure 2. Flavor composition of neutrino mass eigenstates in (3+2) sterile neutrino models. The hatched rectangles indicate active flavor content (electron, muon, tau, respectively, from left to right), and the empty rectangles indicate sterile flavor content.

effect on the final solution. The blue (orange) lines are the solutions to ρ_{ss} (ρ_{pp}) when some of the approximations are not taken. The dashed lines refer to the case when the momentum dependence is taken into account, the dot-dashed lines represent the case when the exact form of the effective potential is considered and the solid lines depict the case when both the momentum spread and the exact form of the potential are assumed. As one can see the effects are relatively small and hence we are confident that the results we obtain are accurate enough for our purposes. Finally, let us note that we have also checked the perfect agreement (in this limit) between the semi-analytic solutions of Eq. (28) and the numerical ones of Eq. (6).

3. Data Samples and Analysis Procedure

We now consider the signatures of the heavy mostly-sterile neutrinos in neutrino oscillation experiments and we study the sterile neutrino production in the Early Universe with a detailed numerical simulation. The results of this simulation are valid both for the ρ_{ss} , $\rho_{pp} \ll \rho_{eq}$ case discussed above, as well as for the case where sterile neutrinos reach thermal abundances (ρ_{ss} , $\rho_{pp} \sim \rho_{eq}$).

A schematic representation of (3+2) models considered in this analysis is shown in Fig. 2. We take a simplified form for the 5×5 mixing matrix, requiring no mixing with the τ -neutrino sector. For the two mostly-sterile states, we allow for variable electron and muon flavor content ($|U_{e4}|^2$, $|U_{\mu4}|^2$, $|U_{\mu5}|^2$, $|U_{\mu5}|^2$), and variable neutrino masses m_4 and m_5 , to be constrained by our analysis described below. Concerning the three mostly-active mass eigenstates, we fix the mass and mixing parameters within the regions currently allowed by solar, reactor, atmospheric, and accelerator long-baseline neutrino

experiments. Specifically, we take $m_1 = 0$, $m_2 = \sqrt{8 \times 10^{-5}}$ eV, $m_3 = \sqrt{2.5 \times 10^{-3}}$ eV for the masses [63], and the upper left 3×3 block form given in the following 5×5 mixing matrix:

$$U_{\alpha i} = \begin{pmatrix} 0.81 & 0.55 & 0 & \pm |U_{e4}| & \pm |U_{e5}| \\ -0.51 & 0.51 & 0.70 & \pm |U_{\mu 4}| & \pm |U_{\mu 5}| \\ 0.28 & -0.67 & 0.70 & 0 & 0 \\ 0 & 0 & 0 & 1 & 0 \\ 0 & 0 & 0 & 0 & 1 \end{pmatrix} , \qquad (32)$$

where the index $\alpha = e, \mu, \tau, s, p$ runs over flavor states, the index $i = 1, \dots, 5$ over mass states, and we indicate the two sterile states with the symbols s, p, respectively. The following simplifying assumptions were therefore made: the lightest neutrino mass eigenstate is assumed to be massless; the normal hierarchy for the mostly-active triplet is taken; the mixing angle θ_{13} is taken to be zero, and θ_{12} , θ_{23} are fixed to their current best-fit values [63]; all six Dirac CP-violating phases allowed for 5 neutrino species are assumed to be zero; zero τ content in the 4th and 5th mass eigenstates is assumed; and no mixing between the sterile states $(U_{s5} = U_{p4} = 0)$. All but maybe the first assumption are expected to have a negligible effect; relaxing the m_1 condition would impose stricter bounds on (3+2) models with respect to what reported in the following. We also note that, while do not know explicitly enforce exact unitarity conditions in Eq. (32) \parallel , this is approximately ensured by the smallness of the $(|U_{e4}|^2, |U_{\mu 4}|^2, |U_{e5}|^2,$ $|U_{\mu 5}|^2$) elements, providing a sufficiently accurate description. In summary, our analysis of SBL and cosmological data allows us to constrain six parameters of (3+2) models: the masses m_4 , m_5 , and the mixing matrix elements $|U_{e4}|^2$, $|U_{\mu4}|^2$, $|U_{\mu5}|^2$, $|U_{\mu5}|^2$. In the following, combinations of these six parameters will be shown.

3.1. Short-Baseline Oscillation Data

Our analysis of SBL data follows closely what done in [31, 32]. We consider neutrino and antineutrino data samples for three different oscillations channels: muon-to-electron neutrino transitions, electron neutrino disappearance, and muon neutrino disappearance. Muon-to-electron neutrino data sets considered come from the LSND [25], KARMEN2 [64], and NOMAD [65] experiments. With respect to previous analyses, we also include recent data [66] on the $\nu_{\mu} \rightarrow \nu_{e}$ search by the MiniBooNE experiment [67]. Constraints on electron neutrino disappearance are based on data from the Bugey [68] and CHOOZ [13] reactor experiments, while data from the accelerator-based CDHS [69] and CCFR [70] experiments were used for muon neutrino disappearance. In addition, muon neutrino disappearance is constrained also by atmospheric [7, 8] and long-baseline [10] data, as done in [71]. The SBL experimental input used is summarized in Tab. 1.

Given the baselines and neutrino energies available to the short-baseline experiments described above, it is possible to constrain oscillation frequencies in the

| Experiment | Oscillation Channel | L/E (km/GeV) | Data Points |
|------------|-----------------------------------|---------------|-------------|
| KARMEN2 | $\nu_{\mu} \rightarrow \nu_{e}$ | 0.3-1.1 | 9 |
| LSND | | 0.5 - 1.4 | 5 |
| MiniBooNE | | 0.2 - 1.1 | 8 |
| NOMAD | | 0.002 - 0.3 | 30 |
| Bugey | $ u_e \rightarrow \nu_e $ | 2-50 | 60 |
| CHOOZ | | 100-400 | 14 |
| CCFR | $ u_{\mu} \rightarrow \nu_{\mu} $ | 0.004-0.03 | 18 |
| CDHS | | 0.02 - 1.5 | 15 |

Table 1. Summary of SBL data used in this analysis.

| Data Set | $m_4 \text{ (eV)}$ | $m_5 \text{ (eV)}$ | U_{e4} | $U_{\mu 4}$ | U_{e5} | $U_{\mu 5}$ |
|-----------|--------------------|--------------------|------------------------|---------------------|-----------------------|-------------|
| SBL-only | 0.96 | 5.0 | 0.12 | 0.15 | 0.59×10^{-1} | 0.16 |
| SBL+cosmo | 0.68 | 0.95 | -0.37×10^{-1} | 0.77×10^{-2} | 0.13 | 0.19 |

Table 2. Summary of (3+2) model best-fit mass and mixing parameters. Top row using SBL data only and bottom row for a combined fit of both SBL and cosmological data.

LSND allowed region, i.e., $\Delta m^2 \sim 1 \text{ eV}^2$, as well as the corresponding oscillation amplitudes involving electron and muon neutrino flavors. Data are fitted to the (3+2) appearance and disappearance oscillation probabilities applicable for short baseline experiments and described in [31, 32], allowing to extract allowed regions in the six-dimensional mass and mixing parameter space considered in this analysis. Parameter values that best describe SBL data are given in the top row of Tab. 2.

3.2. Cosmological Data and Model

With the advent of the modern CMB datasets, such as those coming from experiments like WMAP [72], Boomerang [73] and ACBAR [74] data, combined with modern galaxy surveys, for example SDSS and 2dF surveys, cosmology has entered a precision era in which not only basic cosmological parameters can be constrained, but also fundamental physical parameters that enter the theory.

Cosmological neutrinos have a profound impact on cosmology since they change the expansion history of the Universe and affect the growth of perturbations [75]. Cosmological probes are sensitive to the number of neutrinos, their relative masses and abundances. In order to get theoretical predictions for cosmological datasets, Boltzmann codes must be used that follow the cosmological perturbation evolution in the linear regime, accurately accounting, in addition to the standard cosmological constituents, for each neutrino species. In this work we use the popular package cosmomc [76], which has been adapted to work with more than one massive neutrino species.

Our basic cosmological model is the minimal inflationary Λ CDM model that is consistent with most standard cosmological probes. In addition to neutrino parameters

discussed below, its parameters are the baryon density expressed as a fraction of the critical density multiplied by h^2 , $\omega_b = \Omega_b h^2$, where $h = H_0/100 {\rm km/s/Mpc}$ is the reduced Hubble constant H_0 , same for the cold dark matter $\omega_{\rm dm} = \Omega_{\rm dm} h^2$, the ratio of sound horizon to the angular diameter distance θ , which is essentially a proxy for the Hubble constant, the optical depth to the last scattering τ , logarithm of amplitude $\log A$ and spectral index of primordial fluctuations n_s . These basic parameters are enough to provide a good fit to all available data and set other parameters. For example, the dark energy density in a flat Universe is simply given by $\Omega_{\Lambda} = 1 - \Omega_b - \Omega_{\rm dm}$.

The cosmomc code has been expanded to include 5 species of neutrinos. We assume that their masses are given by

$$m_i = (0.9 \times 10^{-3} \text{eV}, 5 \times 10^{-2} \text{eV}, m_4, m_5)$$
 (33)

and abundances by

$$a_i = (1, 1, 1, a_4, a_5).$$
 (34)

This results in four extra parameters, $m_{4,5}$ and $a_{4,5}$, on top of those that set the basic cosmological model. In principle, indices 4 and 5 are interchangeable and therefore likelihood space is symmetric with respect to this change. We do not attempt to change the parametrization to account for that, but instead use the symmetry as an additional check for chain convergence. We use a flat prior between zero and unity for the abundance parameter a_i . Since at zero abundance, the mass can take any value, we limit the masses to be less than 20 eV. In practice, this upper limit is not relevant for the abundances and masses of interest.

On the data side, we start with a conservative compendium of cosmological datasets. These include the standard cosmic microwave background data, namely WMAP 5-year data [15, 72], Boomerang 03 data [73], the latest ACBAR data [74] and the VSA data [77]. In addition we use the data on the matter power spectrum from the spectroscopic survey of Luminous Red Galaxies (LRGs) from the SDSS survey [78]. To constrain the basic model, we also use the constraints coming from the latest compilation of supernovae [79]. Finally, we also apply the prior on the reduced Hubble constant of $h = 0.72 \pm 0.08$ from the Hubble key project [80].

The basic cosmological model and the basic parameter set is what we use throughout the paper and it represents conservative constraints from the minimal cosmological model. The check the sensitivity of our constraints on the model used, we also calculate constraints on an expanded model, in which we also vary the total energy density of the Universe, or equivalently the curvature, parametrized by $\Omega_k = 1 - \sum \Omega_i$, where the index i runs over the various components of the Universe and the parameter w (pressure over density) that describes the equation of state of the dark energy. In the concordance model, these two parameters have values zero and -1, respectively. On the other hand, we also use cosmological data more aggressively and use the Lyman- α forest data from the SDSS quasar sample (see e.g. [20]). This dataset provides very good constraints on the neutrino properties and has no known systematics at the moment, but it is an extremely difficult experiment that has proven to be somewhat controversial.

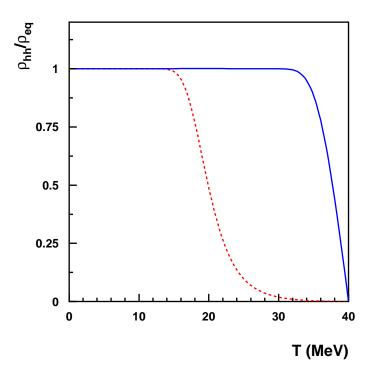


Figure 3. Evolution of sterile neutrino abundances, normalized to thermal equilibrium abundances $\rho_{\rm eq}$, as a function of temperature T. The dashed red (solid blue) line indicate $\rho_{ss}/\rho_{\rm eq}$ ($\rho_{pp}/\rho_{\rm eq}$). The case shown corresponds to the (3+2) model that describes SBL-only data best.

3.3. Analysis Procedure

In practice, we proceed as follows. First, we generate via a MCMC method a large number of (3+2) models that give a potentially viable description of SBL data. Specifically, in this analysis we use about 1.6×10^4 models characterized by a SBL goodness-of-fit within about $20 \chi^2$ units of the SBL best-fit. Second, for each one of those models, we determine the cosmological sterile neutrino abundances as described in Sec. 2. As one example, we show in Fig. 3 the behavior of the sterile neutrino abundances, normalized to the abundance at thermal equilibrium, as obtained by our analysis for the (3+2) model that describes SBL data best (see top row of Tab. 2). Fig. 3 shows the evolution of ρ_{ss}/ρ_{eq} and ρ_{pp}/ρ_{eq} as the temperature of the thermal bath decreases, starting with null abundances at T=40 MeV (right side of plot). For the SBL best-fit model, one can see from Fig. 3 that both sterile neutrino states reach thermal abundances before decoupling. In other words, in this case, their masses fully contribute to the sterile neutrino matter density $(\Omega_s + \Omega_p)h^2$. Third, the viability for each of the models considered is further assessed by contrasting the predicted sterile neutrino abundances with cosmological observations, as explained next.

In order to combine the short-baseline oscillation data with the cosmological constraints, we first run extremely deep MCMC with about 70 - 100 thousands *accepted* samples. Each sample is sampled from the combined probability density in the N-

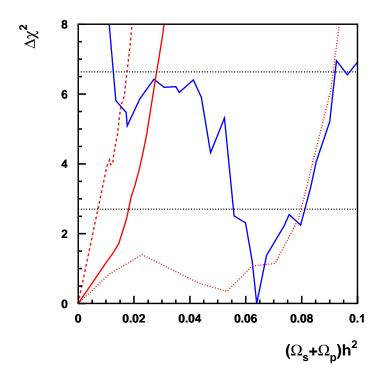


Figure 4. $\Delta \chi^2$ profiles as a function of the sterile neutrino matter density $(\Omega_s + \Omega_p)h^2$. The red (blue) line indicates the case where cosmological-only (SBL-only) data are fitted. Three scenarios are shown for cosmological data fits: default data set and model (solid), data set including Lyman- α forest data and default model (dashed), default data set and cosmological model with free w and Ω_k (dotted). The horizontal dotted lines define the 90% and 99% confidence level regions (1 dof).

dimensional parameter space. The density of samples, projected to the 4-dimensional hyper-cube of parameters (m_4, m_5, a_4, a_5) , thus corresponds to the probability density for those parameters, marginalized over the remaining cosmological parameters, which are, for the sake of this work, nuisance parameters. The relative probability of any model with some finite 4th and 5th neutrino masses and abundances relative to the standard minimal 3-neutrino model is calculated by comparing the relative densities of samples at the considered model position in the sample to the densities in the $(a_4, a_5) = (0, 0)$ corner of the parameter space. We calculate the local densities of samples in spheres (which might be cut by the edge of the parameter space, but this is taken into account). These are then converted to the likelihood ratios, which are in turn converted to the effective $\Delta \chi^2$. This procedure allows us to importance-sample the MCMC from the short-baseline oscillation data in Sec. 3.1.

4. Results

Two types of results are presented. First, in Sec. 4.1, we quantitatively address the compatibility of the SBL (including LSND and MiniBooNE) and cosmological data sets. Second, in Sec. 4.2, we perform a combined analysis of SBL and cosmological data. In

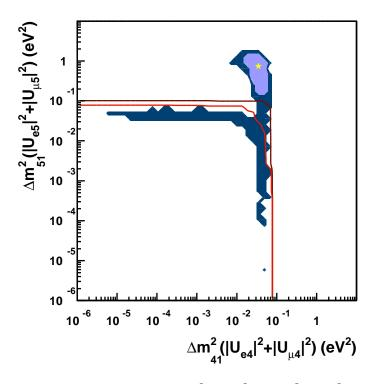


Figure 5. Allowed regions in $(\Delta m_{41}^2(|U_{e4}|^2 + |U_{\mu4}|^2), \Delta m_{51}^2(|U_{e5}|^2 + |U_{\mu5}|^2))$ space, for SBL-only data (filled blue regions) and cosmology-only data (red contours). Light (dark) colors correspond to 90% (99%) confidence level regions (2 dof). The yellow star indicates the SBL-only best-fit point.

both cases, the analysis is carried out under a (3 + 2) sterile neutrino hypothesis (see Sec. 3) and using the multi-flavor description of cosmological sterile neutrino abundances (see Sec. 2).

4.1. Data Sets Compatibility

Fig. 4 shows how the χ^2 for the SBL and cosmology data sets separately vary as a function of the sterile neutrino matter density $(\Omega_s + \Omega_p)h^2$. The χ^2 profiles for both data sets are shown relative to their respective best-fit χ^2 values. Cosmological data prefers a small (if non-zero) value for $(\Omega_s + \Omega_p)h^2$, while SBL data is not consistent with a null $(\Omega_s + \Omega_p)h^2$ value, since the LSND $\bar{\nu}_e$ excess cannot be interpreted in terms of neutrino oscillations in this case. Quantitatively, we find the following allowed intervals, with confidence levels for 1 degree of freedom (dof) given:

- Cosmology: $(\Omega_s + \Omega_p)h^2 < 0.018 (90\% \text{ CL}), (\Omega_s + \Omega_p)h^2 < 0.028 (99\% \text{ CL})$
- SBL: $0.055 < (\Omega_s + \Omega_p)h^2 < 0.081$ (90% CL), $0.013 < (\Omega_s + \Omega_p)h^2 < 0.097$ (99% CL)

In other words, no overlap is found at 90% CL in the $(\Omega_s + \Omega_p)h^2$ ranges allowed by the two data sets, while overlap exists at 99% CL.

The previous numbers refer to our default cosmological data set and default cosmological model described in Sec. 3.2, the one used as reference for all following

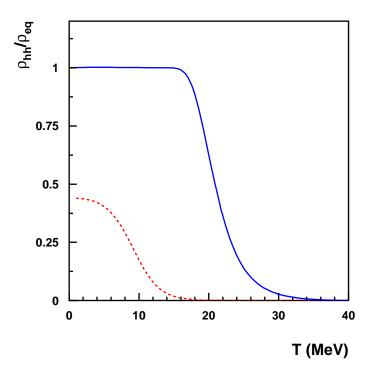


Figure 6. Evolution of sterile neutrino abundances, normalized to thermal equilibrium abundances $\rho_{\rm eq}$, as a function of temperature T. The dashed red (solid blue) line indicate $\rho_{ss}/\rho_{\rm eq}$ ($\rho_{pp}/\rho_{\rm eq}$). The case shown corresponds to the (3+2) model that describes all data (SBL plus cosmology) best.

results and figures. In Fig. 4, this case corresponds to the solid red line. We have also investigated the impact of varying the cosmological data set and cosmological model. The dashed red line in Fig. 4 uses an extended data set including Lyman- α forest data, providing a tighter cosmological constraint. On the other hand, the dotted red line in Fig. 4 quantifies by how much the cosmological constraint is relaxed by assuming a cosmological model with free w and Ω_k (see Sec. 3.2).

Fig. 5 conveys similar compatibility information as the one shown in Fig. 4, but expressed in terms of particle physics rather than cosmological parameters. Two-dimensional allowed regions in $(\Delta m_{41}^2(|U_{e4}|^2+|U_{\mu4}|^2),\Delta m_{51}^2(|U_{e5}|^2+|U_{\mu5}|^2))$ are shown, separately for the SBL and cosmological data sets. As the neutrino masses and/or the electron plus muon flavor of the two heavy (mostly-sterile) states increases, the heavy neutrino matter density $(\Omega_s + \Omega_p)h^2$ tends to increase, either because of the larger neutrino mass or because of a more fully thermalized abundance. Overlap is found between the regions allowed by SBL and cosmology only at 99%, but not at 90%, confidence level (2 dof). Given the cosmological constraints on $(\Omega_s + \Omega_p)h^2$ in Fig. 4, we note that the corresponding bounds on $\Delta m_{j1}^2 \sum_a U_{aj}^2$, with j=4,5 and shown in Fig. 5, are in this case about two orders of magnitude less stringent compared to what would have been expected from Eq. 31. As previously mentioned, the reason is that Eq. 31 is only applicable for ρ_{ss} , $\rho_{pp} \ll \rho_{eq}$ and is not generally valid in this case.

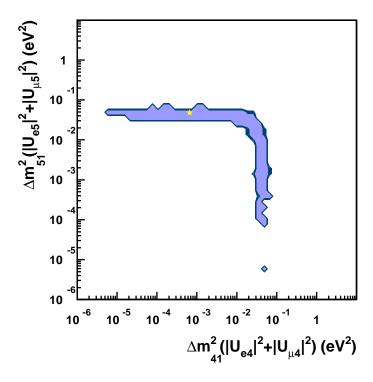


Figure 7. Allowed regions in $(\Delta m_{41}^2(|U_{e4}|^2 + |U_{\mu4}|^2), \Delta m_{51}^2(|U_{e5}|^2 + |U_{\mu5}|^2))$ space, for all data (SBL plus cosmology). Light (dark) blue regions correspond to 90% (99%) confidence level (2 dof). The yellow star indicates the global best-fit point.

As an additional statistical test for compatibility, we consider the "parameter goodness-of-fit" (PG) defined in [81]. The test allows to quantify how likely it is that SBL and cosmological results arise from the same underlying (3+2) sterile neutrino This method alleviates a problem affecting goodness-of-fit tests based on absolute χ^2 values, namely that a possible disagreement between the two data sets is diluted by data points which are insensitive to the parameters that are common to both data sets. The number of parameters common to both data sets is 4 in our case, since cosmological data only depend on (m_4, m_5, a_4, a_5) , where the sterile neutrino abundances a_4 and a_5 defined in Sec. 3.2 are complicated functions of all mass and mixing parameters. This is because, in general, we cannot assume the sterile neutrinos to thermalize, and therefore the mixing matrix elements (in addition to the neutrino masses) play a role in the cosmological case also. The test is based on the statistic $\chi^2_{\rm PG} = \chi^2_{\rm PG,\; cosmo} + \chi^2_{\rm PG,\; SBL}, \text{ where } \chi^2_{\rm PG,\; cosmo} \equiv (\chi^2_{\rm cosmo})_{\rm all\; min} - (\chi^2_{\rm cosmo})_{\rm cosmo\; min} \text{ and } \chi^2_{\rm PG}$ $\chi^2_{\rm PG,~SBL} \equiv (\chi^2_{\rm SBL})_{\rm all~min} - (\chi^2_{\rm SBL})_{\rm SBL~min}$ are the (positive) differences for the cosmology and SBL χ^2 values obtained by minimizing the combined (cosmology plus SBL) χ^2 function discussed in Sec. 4.2, minus the χ^2 values that best fit the two individual data sets. In our case, we obtain $\chi^2_{\rm PG,\ cosmo}=1.71$ and $\chi^2_{\rm PG,\ SBL}=5.81,$ yielding $\chi^2_{\rm PG} = 7.52$. The goodness of fit parameter corresponding to this $\chi^2_{\rm PG}$ value and four common parameters gives a 11.1% compatibility between the two data sets.

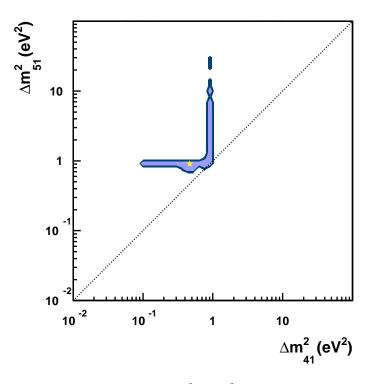


Figure 8. Allowed regions in $(\Delta m_{41}^2, \Delta m_{51}^2)$ space, for all data (SBL plus cosmology). Light (dark) blue regions correspond to 90% (99%) confidence level (2 dof). The dotted line indicates $\Delta m_{41}^2 = \Delta m_{51}^2$. The conventional choice $\Delta m_{41}^2 > \Delta m_{51}^2$ is adopted in this analysis. The yellow star indicates the global best-fit point.

4.2. Joint Analysis

Assuming that SBL and cosmological measurements arise from the same underlying (3+2) sterile neutrino model, we have also performed a combined analysis, where the function to be minimized is the sum of the SBL and cosmology χ^2 functions. The best-fit parameters for this combined analysis are given in the bottom row of Tab. 2. As expected, the inclusion of cosmological data tends to prefer smaller sterile neutrino masses, compared to the SBL-only case. In addition, the best-fit mixing matrix elements are such as to alter the thermalization of the lowest mass sterile state. This is illustrated in Fig. 6, which is the equivalent of Fig. 3 for the best-fit SBL+cosmological model, rather than for the SBL-only analysis. In this case, the fourth mass state decouples with a density of only about 44% of the thermal one.

Allowed regions in $(\Delta m_{41}^2(|U_{e4}|^2 + |U_{\mu4}|^2), \Delta m_{51}^2(|U_{e5}|^2 + |U_{\mu5}|^2))$ space from the combined analysis are shown in Fig. 7. As expected, the allowed region in the top-right portion of Fig. 5 disappears with the inclusion of cosmological data in the fit, reducing the parameter space allowed to the overlap region between the SBL and cosmological regions.

Figs. 8 and 9 show additional two-dimensional projections of the six-dimensional parameter space allowed by the combined analysis. Fig. 8 illustrates allowed values for the fourth and fifth mass states of (3 + 2) models, and Fig. 9 their total active flavor

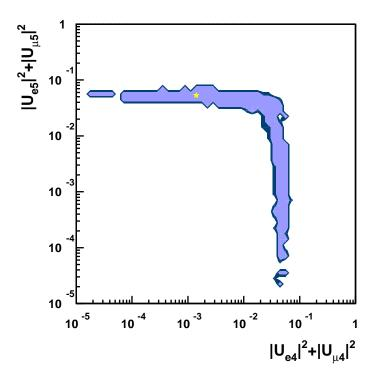


Figure 9. Allowed regions in $(|U_{e4}|^2 + |U_{\mu4}|^2, |U_{e5}|^2 + |U_{\mu5}|^2)$ space, for all data (SBL plus cosmology). Light (dark) blue regions correspond to 90% (99%) confidence level (2 dof). The yellow star indicates the global best-fit point.

content (electron plus muon). In these figures, we can see that favored (3 + 2) sterile neutrino models are characterized by one mostly-sterile state that is highly constrained, with $\Delta m_{j1}^2 \sim 1 \text{ eV}^2$, and electron plus muon flavor content of about 5%. On the other hand, mass and mixing parameters for the second mostly-sterile state are far less constrained, with mass splittings in the range 0.1-10 eV², and electron plus muon flavor content in the range 10^{-5} -5 × 10^{-2} .

5. Conclusions

Right-handed, sterile neutrinos can be produced in the Early Universe via active-sterile neutrino oscillations. Depending on the structure of the neutrino mixing matrix and the neutrino masses involved, sterile neutrino production can be copious. In this case, sterile neutrinos are expected to leave a clear imprint on cosmological observables, as active neutrinos do. Given the impressive accuracy reached by recent cosmological probes on one side, and the well-defined nature of the cosmological concordance model capable of interpreting those data on the other side, it is now possible to use the Universe to constrain sterile neutrino properties that have traditionally been probed via laboratory-based neutrino sources.

As already extensively studied in the literature, we take into account how both neutrino interactions with the primeval medium, and neutrino coherence breaking effects, affect the evolution of sterile neutrino abundances [43, 54, 58]. Most previous work generally considers only the simplest sterile neutrino mixing matrix structures possible, that involves mixing a single sterile neutrino species with one or more active species [23]. In this paper we take a more general approach. We generalize those results to account for all mixing effects arising when multiple sterile neutrino flavors participate in the oscillations. Indeed, once sterile neutrinos are added to the Standard Model fermion content, there is no fundamental reason to expect only sterile single-flavor mixing effects.

In addition to full numerical results that are valid, to a good approximation, for generic sterile neutrino models (with the only requirement of relativistic decoupling of sterile neutrinos), we try to emphasize the underlying physics by developing an analytical description that is applicable for sterile neutrinos that are significantly more massive than the active ones, for a mixing matrix that is approximately block-diagonal in its active and sterile sectors, and for sub-thermal sterile neutrino abundances at decoupling. In the latter case, we obtain the following three main results, valid for any number of sterile neutrino species: first, that the production of sterile neutrinos arises entirely from the breaking of the coherence of the evolution of active neutrinos; second, that each active flavor contributes independently to the sterile neutrino abundances; and third, that the evolution of the abundances of distinct sterile neutrino species is independent from one another, in absence of mixing in the sterile sector.

Within our full multi-flavor framework, we have also studied in detail the phenomenology of the so-called (3+2) sterile neutrino models [30, 31]. Two additional heavy (mostly-sterile) neutrino states with masses in the eV range, beyond the minimal three active neutrino mixing scenario, and with small amounts of electron and muon flavor content, are considered in this case. These (3+2) models were originally introduced as a means to reconcile via standard $\bar{\nu}_{\mu} \to \bar{\nu}_{e}$ oscillations the currently unexplained $\bar{\nu}_{e}$ excess observed by the LSND experiment with the solar and atmospheric oscillation signatures. We first study the sterile neutrino evolution in the Early Universe of (3+2) models that offer a potentially viable explanation of all short-baseline oscillation data, including the LSND excess and first $\nu_{\mu} \to \nu_{e}$ results recently released by the MiniBooNE Collaboration. We then contrast the expected energy density of the Universe in the form of sterile neutrinos obtained by those models with the latest cosmological observations coming from cosmic microwave background datasets and galaxy surveys, mostly (but not only) in the framework of the minimal Λ CDM cosmological model.

In contrast with some literature, we find that fully solving the neutrino kinetic equations is necessary even for the relatively large active-sterile mixing implied by this class of models, since sterile neutrino states do not always feature thermal abundances at decoupling. This result, valid for the minimal Λ CDM cosmological model, should be taken into account in future studies on sterile neutrino production in the Early Universe, in order to avoid possibly misleading conclusions. We find that the (3+2) model that best describes short-baseline oscillation data is excluded at high confidence

level by cosmological observations, which do not allow for large amounts of energy density in the form of relativistic species in addition to the energy density of active neutrinos, unless non-minimal Λ CDM models are used. Nevertheless, by fully exploring the neutrino parameter space, we do find (3+2) sterile neutrino models that provide a perfectly acceptable description of short-baseline and cosmological data simultaneously, with a 11% probability for compatibility between the two datasets. As a consequence, we conclude that (3+2) models are significantly more disfavored by the internal inconsistencies between sterile neutrino interpretations of appearance and disappearance short-baseline data themselves [33], rather than by the used cosmological data. Finally, a global analysis of all short-baseline plus cosmological data allow us to further constrain the (3+2) neutrino parameter space, in a region that should be accessible by future experiments aiming to study neutrinos, both the ones permeating the cosmos and neutrinos produced on Earth.

Acknowledgments

OM is supported by a Ramón y Cajal contract from the Spanish Government. SPR is supported by the Portuguese FCT through the projects POCI/FP/81919/2007 and CFTP-FCT UNIT 777, which are partially funded through POCTI (FEDER). SPR is also partially supported by the Spanish Grant FPA2005-01678 of the MCT. MS would like to acknowledge support by the Spanish Ministry of Science and Innovation via a CSIC JAE-DOC contract, and use of the computing cluster of the experimental neutrino group at IFIC for this work.

References

- Fukuda Y et al. [Kamiokande Collaboration], Solar neutrino data covering solar cycle 22, 1996
 Phys. Rev. Lett. 77 1683; Cleveland B T et al., Measurement Of The Solar Electron Neutrino
 Flux With The Homestake Chlorine Detector, 1998 Astrophys. J. 496 505; Hampel W et al.
 [GALLEX Collaboration], GALLEX solar neutrino observations: Results for GALLEX IV, 1999
 Phys. Lett. B 447 127; Abdurashitov J N et al. [SAGE Collaboration], Measurement of the
 solar neutrino capture rate by the Russian-American gallium solar neutrino experiment during
 one half of the 22-year cycle of solar activity, 2002 J. Exp. Theor. Phys. 95 181 [2002 Zh. Eksp.
 Teor. Fiz. 122 211] [arXiv:astro-ph/0204245]; Kirsten T A [GNO Collaboration], Progress in
 GNO, 2003 Nucl. Phys. Proc. Suppl. 118 33.
- [2] Fukuda S et al. [Super-Kamiokande Collaboration], Determination of solar neutrino oscillation parameters using 1496 days of Super-Kamiokande-I data, 2002 Phys. Lett. B 539 179 [arXiv:hep-ex/0205075]; Cravens J P et al. [Super-Kamiokande Collaboration], Solar neutrino measurements in Super-Kamiokande-II, 2008 Phys. Rev. D 78 032002 [arXiv:0803.4312 [hep-ex]].
- [3] Ahmad Q R et al. [SNO Collaboration], Measurement of the charged current interactions produced by B-8 solar neutrinos at the Sudbury Neutrino Observatory, 2001 Phys. Rev. Lett. 87 071301 [arXiv:nucl-ex/0106015].
- [4] Ahmad Q R et al. [SNO Collaboration], Direct evidence for neutrino flavor transformation from neutral-current interactions in the Sudbury Neutrino Observatory, 2002 Phys. Rev. Lett. 89

- 011301 [arXiv:nucl-ex/0204008]; Measurement of day and night neutrino energy spectra at SNO and constraints on neutrino mixing parameters, ibid. 2002 89 011302 [arXiv:nucl-ex/0204009].
- [5] Ahmed S N et al. [SNO Collaboration], Measurement of the total active B-8 solar neutrino flux at the Sudbury Neutrino Observatory with enhanced neutral current sensitivity, 2004 Phys. Rev. Lett. 92 181301 [arXiv:nucl-ex/0309004].
- [6] Aharmim B et al. [SNO Collaboration], Electron energy spectra, fluxes, and day-night asymmetries of B-8 solar neutrinos from the 391-day salt phase SNO data set, 2005 Phys. Rev. C 72 055502 [arXiv:nucl-ex/0502021].
- [7] Ashie Y et al. [Super-Kamiokande Collaboration], A measurement of atmospheric neutrino oscillation parameters by Super-Kamiokande I, 2005 Phys. Rev. D 71 112005 [arXiv:hep-ex/0501064]. Hosaka J et al. [Super-Kamiokande Collaboration], Three flavor neutrino oscillation analysis of atmospheric neutrinos in Super-Kamiokande, 2006 Phys. Rev. D 74 032002 [arXiv:hep-ex/0604011].
- [8] H. Sekiya for the Super-Kamiokande Collaboration, Recent Results from Super-Kamiokande, arXiv:0810.0595 [astro-ph].
- [9] Abe S et al. [KamLAND Collaboration], Precision Measurement of Neutrino Oscillation Parameters with KamLAND, 2008 Phys. Rev. Lett. 100 221803 [arXiv:0801.4589 [hep-ex]].
- [10] Ahn M H et al. [K2K Collaboration], Measurement of neutrino oscillation by the K2K experiment, 2006 Phys. Rev. D 74 072003 [arXiv:hep-ex/0606032].
- [11] Ables E et al. [MINOS Collaboration], FERMILAB-PROPOSAL-0875.
- [12] Adamson P et al. [MINOS Collaboration], Measurement of Neutrino Oscillations with the MINOS Detectors in the NuMI Beam, Phys. Rev. Lett. 101 (2008) 131802 [arXiv:0806.2237 [hep-ex]]; Search for active neutrino disappearance using neutral-current interactions in the MINOS long-baseline experiment, arXiv:0807.2424 [hep-ex].
- [13] Apollonio M et al. [CHOOZ Collaboration], Limits on neutrino oscillations from the CHOOZ experiment, 1999 Phys. Lett. B 466 415 [arXiv:hep-ex/9907037]; Search for neutrino oscillations on a long base-line at the CHOOZ nuclear power station, 2003 Eur. Phys. J. C 27 331 [arXiv:hep-ex/0301017].
- [14] Boehm F et al., Search for neutrino oscillations at the Palo Verde nuclear reactors, 2000 Phys. Rev. Lett. 84 3764 [arXiv:hep-ex/9912050]; Results from the Palo Verde neutrino oscillation experiment, 2000 Phys. Rev. D 62 072002 [arXiv:hep-ex/0003022].
- [15] Komatsu E et al. [WMAP Collaboration], Five-Year Wilkinson Microwave Anisotropy Probe Observations: Cosmological Interpretation, arXiv:0803.0547 [astro-ph].
- [16] Lesgourgues J and Pastor S, Massive neutrinos and cosmology, 2006 Phys. Rept. 429 307 [arXiv:astro-ph/0603494].
- [17] Spergel D N et al. [WMAP Collaboration], First Year Wilkinson Microwave Anisotropy Probe (WMAP) Observations: Determination of Cosmological Parameters, 2003 Astrophys. J. Suppl. 148 (2003) 175 [arXiv:astro-ph/0302209]; Hannestad S, Neutrino masses and the number of neutrino species from WMAP and 2dFGRS, 2003 JCAP 0305 004 [arXiv:astro-ph/0303076]; Allen S W, Schmidt R W and Bridle S L, A preference for a non-zero neutrino mass from cosmological data, 2003 Mon. Not. Roy. Astron. Soc. 346 593 [arXiv:astro-ph/0306386]; Tegmark M et al. [SDSS Collaboration], Cosmological parameters from SDSS and WMAP, 2004 Phys. Rev. D 69 103501 [arXiv:astro-ph/0310723]; Barger V, Marfatia D and Tregre A, Neutrino mass limits from SDSS, 2dFGRS and WMAP, 2004 Phys. Lett. [arXiv:hep-ph/0312065]; Hannestad S and Raffelt G, Cosmological mass limits on neutrinos, axions, and other light particles, 2004 JCAP 0404 008 [arXiv:hep-ph/0312154]; Brandenberger R H, Mazumdar A and Yamaguchi M, A note on the robustness of the neutrino mass bounds from cosmology, 2004 Phys. Rev. D 69 081301 [arXiv:hep-ph/0401239]; Crotty P, Lesgourgues J and Pastor S, Current cosmological bounds on neutrino masses and relativistic relics, 2004 Phys. Rev. D 69 123007 [arXiv:hep-ph/0402049]; Seljak U et al. [SDSS Collaboration], SDSS galaxy bias from halo mass-bias relation and its cosmological implications, 2005 Phys. Rev.

- D 71 043511 [arXiv:astro-ph/0406594]; Cosmological parameter analysis including SDSS Lyalpha forest and galaxy bias: Constraints on the primordial spectrum of fluctuations, neutrino mass, and dark energy, 2005 Phys. Rev. D 71 103515 [arXiv:astro-ph/0407372]; Fogli G L et al., Observables sensitive to absolute neutrino masses: Constraints and correlations from world neutrino data, 2004 Phys. Rev. D 70 113003 [arXiv:hep-ph/0408045]; Elgaroy O and Lahav O, Neutrino masses from cosmological probes, 2005 New J. Phys. 7 61 [arXiv:hep-ph/0412075]. Kahniashvili T, von Toerne E, Arhipova N A and Ratra B, Neutrino mass limit from galaxy cluster number density evolution, 2005 Phys. Rev. D 71 125009 [arXiv:astro-ph/0503328]; Hannestad S, Neutrino masses and the dark energy equation of state: Relaxing the cosmological neutrino mass bound, 2005 Phys. Rev. Lett. 95 221301 [arXiv:astro-ph/0505551]; Goobar A, Hannestad S, Mortsell E and Tu H, A new bound on the neutrino mass from the SDSS baryon acoustic peak, 2006 JCAP 0606 019 [arXiv:astro-ph/0602155].
- [18] Spergel D N et al. [WMAP Collaboration], Wilkinson Microwave Anisotropy Probe (WMAP) three year results: Implications for cosmology, 2007 Astrophys. J. Suppl. 170 377 [arXiv:astro-ph/0603449]; Seljak U, Slosar A and McDonald P, Cosmological parameters from combining the Lyman-alpha forest with CMB, galaxy clustering and SN constraints, 2006 JCAP 0610 014 [arXiv:astro-ph/0604335]; Hannestad S and Raffelt G G, Neutrino masses and cosmic radiation density: Combined analysis, 2006 JCAP 0611 016 [arXiv:astro-ph/0607101]; Kristiansen J R, Eriksen H K and Elgaroy O, Revised WMAP constraints on neutrino masses and other extensions of the minimal Lambda CDM model, 2006 Phys. Rev. D 74 123005 [arXiv:astro-ph/0608017].
- [19] Dodelson S, Melchiorri A and Slosar A, Is cosmology compatible with sterile neutrinos?, 2006 Phys. Rev. Lett. 97 04301 [arXiv:astro-ph/0511500].
- [20] Fogli G L et al., Observables sensitive to absolute neutrino masses (Addendum), 2008 Phys. Rev. D 78 033010 [arXiv:0805.2517 [hep-ph]].
- [21] Barger V, Kneller J P, Lee H S, Marfatia D and Steigman G, Effective number of neutrinos and baryon asymmetry from BBN and WMAP, 2003 Phys. Lett. B 566 8 [arXiv:hep-ph/0305075]; Barger V, Kneller J P, Langacker P, Marfatia D and Steigman G, Hiding relativistic degrees of freedom in the early universe, 2003 Phys. Lett. B 569 123 [arXiv:hep-ph/0306061]; Cuoco A et al., Present status of primordial nucleosynthesis after WMAP: results from a new BBN code, 2004 Int. J. Mod. Phys. A 19 4431 [arXiv:astro-ph/0307213]; Hannestad S, New constraint on the cosmological background of relativistic particles, 2006 JCAP 0601 001 [arXiv:astro-ph/0510582]; Cirelli M and Strumia A, Cosmology of neutrinos and extra light particles after WMAP3, 2006 JCAP 0612) 013 [arXiv:astro-ph/0607086]; Ichikawa K, Kawasaki M and Takahashi F, Constraint on the Effective Number of Neutrino Species from the WMAP and SDSS LRG Power Spectra, 2007 JCAP 0705 007 [arXiv:astro-ph/0611784].
- [22] Mangano G et al., Present bounds on the relativistic energy density in the Universe from cosmological observables, 2007 JCAP 0703 006 [arXiv:astro-ph/0612150]; Hamann J et al., Observational bounds on the cosmic radiation density, 2007 JCAP 0708 021 [arXiv:0705.0440 [astro-ph]]; Ichikawa K, Sekiguchi T and Takahashi T, Probing the Effective Number of Neutrino Species with Cosmic Microwave Background, Phys. Rev. D 78 (2008) 083526 [arXiv:0803.0889 [astro-ph]]; Simha V and Steigman G, Constraining The Early-Universe Baryon Density And Expansion Rate, 2008 JCAP 0806 016 [arXiv:0803.3465 [astro-ph]].
- [23] Cirelli M, Marandella G, Strumia A and Vissani F, Probing oscillations into sterile neutrinos with cosmology, astrophysics and experiments, 2005 Nucl. Phys. B 708 215 [arXiv:hep-ph/0403158].
- [24] Bilenky S M, Giunti C and Grimus W, Neutrino mass spectrum from the results of neutrino oscillation experiments, 1998 Eur. Phys. J. C 1 247 [arXiv:hep-ph/9607372]; Barger V D, Weiler T J and Whisnant K, Four-way neutrino oscillations, 1998 Phys. Lett. B 427 97 [arXiv:hep-ph/9712495]; Bilenky S M, Giunti C, Grimus W and Schwetz T, Four-neutrino mixing and big-bang nucleosynthesis, 1999 Astropart. Phys. 11 413 [arXiv:hep-ph/9804421]; Barger V D, Pakvasa S, Weiler T J and Whisnant K, Variations on four-neutrino oscillations,

- 1998 Phys. Rev. D **58** 093016 [arXiv:hep-ph/9806328].
- [25] Aguilar A et al. [LSND Collaboration], Evidence for neutrino oscillations from the observation of anti-nu/e appearance in a anti-nu/mu beam, 2001 Phys. Rev. D 64 112007 [arXiv:hep-ex/0104049].
- [26] Gelmini G, Palomares-Ruiz S and Pascoli S, Low reheating temperature and the visible sterile neutrino, 2004 Phys. Rev. Lett. 93 081302 [arXiv:astro-ph/0403323]; Gelmini G, Osoba E, Palomares-Ruiz S and Pascoli S, MeV sterile neutrinos in low reheating temperature cosmological scenarios, 2008 JCAP 0810 029 [arXiv:0803.2735 [astro-ph]].
- [27] Foot R and Volkas R R, Reconciling sterile neutrinos with big bang nucleosynthesis, 1995 Phys. Rev. Lett. 75 4350 [arXiv:hep-ph/9508275].
- [28] Babu K S and Rothstein I Z, Relaxing nucleosynthesis bounds on sterile-neutrinos, 1992 Phys. Lett. B 275 112.
- [29] Bento L and Berezhiani Z, Blocking active-sterile neutrino oscillations in the early universe with a Majoron field, 2001 Phys. Rev. D 64 115015 [arXiv:hep-ph/0108064].
- [30] Peres O L G and Smirnov A Y, (3+1) spectrum of neutrino masses: A chance for LSND?, 2001 Nucl. Phys. B 599 3 [arXiv:hep-ph/0011054].
- [31] Sorel M, Conrad J M and Shaevitz M, A combined analysis of short-baseline neutrino experiments in the (3+1) and (3+2) sterile neutrino oscillation hypotheses, 2004 Phys. Rev. D **70** 073004 [arXiv:hep-ph/0305255].
- [32] Karagiorgi G et al, Leptonic CP violation studies at MiniBooNE in the (3+2) sterile neutrino oscillation hypothesis, 2007 Phys. Rev. D **75** 013011 [arXiv:hep-ph/0609177].
- [33] Maltoni M and Schwetz T, Sterile neutrino oscillations after first MiniBooNE results, 2007 Phys. Rev. D 76 093005 [arXiv:0705.0107 [hep-ph]].
- [34] Barbieri R and Dolgov A, Bounds on Sterile-neutrinos from Nucleosynthesis, 1990 Phys. Lett. B 237 440.
- [35] Enqvist K, Kainulainen K and Maalampi J, Neutrino Asymmetry And Oscillations In The Early Universe, 1990 Phys. Lett. B 244 186.
- [36] Kainulainen K, Light Singlet Neutrinos And The Primordial Nucleosynthesis, 1990 Phys. Lett. B 244 191.
- [37] Enqvist K, Kainulainen K and Maalampi J, Resonant neutrino transitions and nucleosynthesis, 1990 Phys. Lett. B **249** 531.
- [38] Barbieri R and Dolgov A, Neutrino oscillations in the early universe, 1991 Nucl. Phys. B **349** 743.
- [39] Savage M J, Malaney R A and Fuller G M, Neutrino Oscillations and the Leptonic Charge of the Universe, 1991 Astrophys. J. 368 1.
- [40] Enqvist K, Kainulainen K and Thomson M J, Stringent cosmological bounds on inert neutrino mixing, 1992 Nucl. Phys. B 373 498.
- [41] Shi X, Schramm D N and Fields B D, Constraints on neutrino oscillations from big bang nucleosynthesis, 1993 Phys. Rev. D 48 2563 [arXiv:astro-ph/9307027].
- [42] Dodelson S and Widrow L M, Sterile-neutrinos as dark matter, 1994 Phys. Rev. Lett. 72 17 [arXiv:hep-ph/9303287].
- [43] Dolgov A D, Neutrinos In The Early Universe, 1981 Sov. J. Nucl. Phys. 33 700 [1981 Yad. Fiz. 33 1309].
- [44] Khlopov M Y and Petcov S T, Possible cosmological effect of CP violation in neutrino oscillations, 1981 Phys. Lett. B 99 117; Fargion D and Shepkin M G, Does cosmology imply a Dirac neutrino mass?, 1984 Phys. Lett. B 146 46; Langacker P, Sathiapalan B and Steigman G, The Electron-Neutrino Mass, Double Beta Decay, And Cosmology, 1986 Nucl. Phys. B 266 669.
- [45] Langacker P, Petcov S T, Steigman G and Toshev S, On the Mikheev-Smirnov-Wolfenstein (MSW) Mechanism of Amplification of Neutrino Oscillations in Matter, 1987 Nucl. Phys. B 282 589.
- [46] Iocco F, Mangano G, Miele G, Pisanti O and Serpico P D, Primordial Nucleosynthesis: from precision cosmology to fundamental physics, arXiv:0809.0631 [astro-ph].

- [47] Dolgov A D and Villante F L, BBN bounds on active-sterile neutrino mixing, 2004 Nucl. Phys. B 679 261 [arXiv:hep-ph/0308083].
- [48] Harris R A and Stodolsky L, Quantum Beats In Optical Activity And Weak Interactions, 1978 Phys. Lett. B 78 313; On the time dependence of optical activity, 1981 J. Chem. Phys. 74 2145; Two State Systems In Media And 'Turing's Paradox', 1982 Phys. Lett. B 116 464; Thomson M J, The Damping of quantum coherence by elastic and inelastic processes, 1992 Phys. Rev. A 45 2243.
- [49] Stodolsky L, On the Treatment of Neutrino Oscillations in a Thermal Environment, 1987 Phys. Rev. D 36 2273.
- [50] Manohar A, Statistical Mechanics of Noninteracting Particles, 1987 Phys. Lett. 186B 370.
- [51] Thomson M J, McKellar B H J, Univ. of Melbourn preprint, UMP 89-108, Univ. of Manchester preprint, MC-TP-91-1.
- [52] Pantaleone J T, Neutrino oscillations at high densities, 1992 Phys. Lett. B 287 128; Dirac neutrinos in dense matter, 1992 Phys. Rev. D 46 510.
- [53] Raffelt G, Sigl G and Stodolsky L, NonAbelian Boltzmann equation for mixing and decoherence, 1993 Phys. Rev. Lett. 70 2363 [2007 Erratum-ibid. 98 069902] [arXiv:hep-ph/9209276].
- [54] Sigl G and Raffelt G, General kinetic description of relativistic mixed neutrinos, 1993 Nucl. Phys. B 406 423.
- [55] Samuel S, Neutrino oscillations in dense neutrino gases, 1993 Phys. Rev. D 48 1462; Kostelecky V A, Pantaleone J T and Samuel S, Neutrino Oscillation In The Early Universe, 1993 Phys. Lett. B 315 46; Kostelecky V A and Samuel S, Nonlinear Neutrino Oscillations In The Expanding Universe, 1994 Phys. Rev. D 49 1740.
- [56] McKellar B H J and Thomson M J, Oscillating doublet neutrinos in the early universe, 1994 Phys. Rev. D 49 2710.
- [57] Bell N F, Volkas R R and Wong Y Y Y, Relic neutrino asymmetry evolution from first principles, 1999 Phys. Rev. D 59 113001 [arXiv:hep-ph/9809363].
- [58] Dolgov A D, Neutrinos in cosmology, 2002 Phys. Rept. **370** 333 [arXiv:hep-ph/0202122].
- [59] Notzold D and Raffelt G, Neutrino Dispersion at Finite Temperature and Density, 1988 Nucl. Phys. B 307 924.
- [60] Dolgov A D, Hansen S H, Pastor S and Semikoz D V, Neutrino oscillations in the early universe: How large lepton asymmetry can be generated?, 2000 Astropart. Phys. 14 79 [arXiv:hep-ph/9910444].
- [61] Abazajian K, Bell N F, Fuller G M and Wong Y Y Y, Cosmological lepton asymmetry, primordial nucleosynthesis, and sterile neutrinos, 2005 Phys. Rev. D 72 063004 [arXiv:astro-ph/0410175].
- [62] Foot R and Volkas R R, Studies of neutrino asymmetries generated by ordinary sterile neutrino oscillations in the early universe and implications for big bang nucleosynthesis bounds, 1997 Phys. Rev. D 55 5147 [arXiv:hep-ph/9610229].
- [63] Gonzalez-Garcia M C and Maltoni M, Phenomenology with Massive Neutrinos, 2008 Phys. Rept. 460 1 [arXiv:0704.1800 [hep-ph]].
- [64] Armbruster B et al. [KARMEN Collaboration], Upper limits for neutrino oscillations anti-nu/mu

 → anti-nu/e from muon decay at rest, 2002 Phys. Rev. D 65 112001 [arXiv:hep-ex/0203021].
- [65] Astier P et al. [NOMAD Collaboration], Search for nu/mu → nu/e oscillations in the NOMAD experiment, 2003 Phys. Lett. B 570 19 [arXiv:hep-ex/0306037]; Gibin D, Search For Nu/Mu ¡-¿ Nu/E Oscillations In The Nomad Experiment, 1998 Nucl. Phys. Proc. Suppl. 66 366; Valuev V [NOMAD Collaboration], Search for nu/mu → nu/e oscillations in the NOMAD experiment, 2001 J. High Energy Phys. Conf. Proc. PRHEP-hep2001/190.
- [66] For details about MiniBooNE data used, see: http://www-boone.fnal.gov/for_physicists/april07datarelease/
- [67] Aguilar-Arevalo A A et al. [The MiniBooNE Collaboration], A Search for electron neutrino appearance at the $\Delta m^2 \sim 1 \mathrm{eV}^2$ scale, 2007 Phys. Rev. Lett. **98** 231801 [arXiv:0704.1500 [hep-ex]].

- [68] Declais Y et al., Search for neutrino oscillations at 15-meters, 40-meters, and 95-meters from a nuclear power reactor at Bugey, 1995 Nucl. Phys. B 434 503.
- [69] Dydak F et al., A Search For Muon-Neutrino Oscillations In The Delta M**2 Range 0.3-Ev**2 To 90-Ev**2, 1984 Phys. Lett. B 134 281.
- [70] Stockdale I E et al., Limits On Muon Neutrino Oscillations In The Mass Range 55-Ev**2; Delta M**2; 800-Ev**2, 1984 Phys. Rev. Lett. 52 1384.
- [71] Maltoni M, Schwetz T, Tortola M A and Valle J W F, Status of global fits to neutrino oscillations, 2004 New J. Phys. 6 122 [arXiv:hep-ph/0405172].
- [72] Dunkley J et al. [WMAP Collaboration], Five-Year Wilkinson Microwave Anisotropy Probe Observations: Likelihoods and Parameters from the WMAP data, arXiv:0803.0586 [astro-ph].
- [73] MacTavish C J et al. [BOOMERANG Collaboration], Cosmological parameters from the 2003 flight of BOOMERANG, 2006 Astrophys. J. 647 799 [arXiv:astro-ph/0507503].
- [74] Reichardt C L et al. [ACBAR Collaboration], High resolution CMB power spectrum from the complete ACBAR data set, arXiv:0801.1491 [astro-ph].
- [75] Bashinsky S and Seljak U, Signatures of relativistic neutrinos in CMB anisotropy and matter clustering, 2004 Phys. Rev. D 69 083002 [arXiv:astro-ph/0310198].
- [76] Lewis A and Bridle S, Cosmological parameters from CMB and other data: a Monte-Carlo approach, 2002 Phys. Rev. D 66 103511 [arXiv:astro-ph/0205436]. Available at cosmologist.info.
- [77] Dickinson Cet al. [VSA Collaboration], High sensitivity measurements of the CMB power spectrum with the extended Very Small Array, 2004 Mon. Not. Roy. Astron. Soc. 353 732 [arXiv:astro-ph/0402498].
- [78] Tegmark M et al. [SDSS Collaboration], Cosmological Constraints from the SDSS Luminous Red Galaxies, 2006 Phys. Rev. D 74 123507 [arXiv:astro-ph/0608632].
- [79] Kowalski M et al., Improved Cosmological Constraints from New, Old and Combined Supernova Datasets, arXiv:0804.4142 [astro-ph].
- [80] Freedman W L et al. [HST Collaboration], Final Results from the Hubble Space Telescope Key Project to Measure the Hubble Constant, 2001 Astrophys. J. **553** 47 [arXiv:astro-ph/0012376].
- [81] Maltoni M and Schwetz T, Testing the statistical compatibility of independent data sets, 2003 Phys. Rev. D 68 033020 [arXiv:hep-ph/0304176].